Effects of pH on Metals Precipitation and Sorption: Field Bioremediation and Geochemical Modeling Approaches

Ming-Kuo Lee* and James A. Saunders

ABSTRACT

At the Sanders Lead car-battery recycling plant, near Troy, AL, groundwater is highly acidic (pH varies from 3 to 3.5) and carries high concentrations of Pb, Cd, Zn, Cu, and Fe. Pilot field experiments conducted at the site show that in situ metabolism of sulfate reducing bacteria (SRB) can produce desired geochemical effects to remove heavy metal Pb, Cd, Zn, and Cu from groundwater. A reaction path model of sulfate reduction shows the redox potential (Eh) effects on mineral precipitation and pH controls on the sorption of different metals. Lead strongly adsorbs to hydrous ferric oxide (HFO) present in the aquifer over a wide pH range. Both sorption (due to pH increase) and solid sulfide formation are important for removing Pb. Although theoretical modeling shows that the sorption of most cations is promoted as pH increases, HFO can only scavenge Zn, Cd, Co, and Ni at relatively neutral pH conditions. Thus concentrations of our primary contaminants Zn and Cd attenuate in acidic conditions primarily via precipitation or coprecipitation of solid sulfide phase as Eh drops. The modeling result explains why the Pb plume is retarded in migration with respect to the Cd plume under the low-pH conditions at the site. For As, arsenate sorbs strongly onto the protonated weak sites of ferric hydroxide for the pH range of calculation. Arsenite sorption is also favored by increasing pH, however, arsenite desorbs and becomes mobilized at very low oxidation state as it reacts with dissolved sulfide to form AsS complexes. In addition, intermittent rainfall events could cause short-term Eh increases, potentially leading to oxidation of sulfide solids and subsequent pH decrease, and the remobilization of metals. This study argues for the importance of accounting for pH changes when evaluating the fate, transport, and long-term stability of metals at shallow contaminated sites.

A SHALLOW UNCONFINED AQUIFER below a car battery recycling plant in Troy, AL is heavily contaminated with heavy metals and sulfate from sulfuric acid spills (Saunders et al., 2001). To assess the feasibility of bioremediation at this site, a field pilot study began in December 1999 as an alternative to an on-going pump-and-treat remediation that proved to be ineffective. The objective of the field experiment was to inject required nutrients to stimulate the growth and metabolic activity of SRB that we hypothesized existed in groundwater even under aerobic and low-pH conditions (see Postgate, 1979; Elliott et al., 1998; Edwards et al., 2000). We further hypothesized that sulfate reduction could be stimulated to the point where amorphous solid sulfide phases would precipitate, leading to metal removals by coprecipitation in solids. This study documents the principal biogeochemical processes that occur at the test site after the injection of bacteria-stimulating solutions. We tracked the changes in water chemistry (major and trace elements, S isotope compositions, pH, Eh) and identified solid "mineral" phases produced by biochemical processes. Theoretical geochemical modeling was conducted to predict how the water chemistry evolves, which minerals precipitate, and how ferric hydroxides adsorb metals during the bioremediation experiment. The modeling results were compared with field observations of changes in water chemistry and precipitations of solid materials after the injection.

In the past few decades hydrogeologists have developed geochemical models, with varying degrees of sophistication, to study water–rock interaction in natural systems (e.g., Helgeson et al., 1970; Wolery, 1979; Reed, 1982; Parkhurst et al., 1990; Bethke, 1996). The purpose of constructing geochemical models is to quantify the chemical and biologic processes that could significantly impact water chemistry in hydrologic systems. Hydrogeologists have spent less effort in predicting the fate and transformation of heavy metals during artificially induced (or engineered) bioremediation, even though the chemical evolution of water provides perhaps the best opportunity to monitor the subsurface remediation processes. We present how a reaction path model could be constructed to trace geochemical evolution (e.g., speciation, mineral precipitation, sorption) of groundwater and sediments during in situ bioremediation experiments conducted at the Troy site. Geochemist's Workbench (Rockware, Inc., Golden, CO) (Bethke, 1996; Lee and Bethke, 1996) was used to investigate how bacteria sulfate reduction induces the precipitation of metal sulfides from the contaminated groundwater. It is well known that bacteria sulfate reduction would produce desired geochemical effects including an increase in pH (e.g., Berner, 1970; Chapelle, 1993; Bottrell et al., 1995). Since the primary control on the process of metal attenuation is acid neutralization, our calculations were aimed at predicting the pH range at which adsorption of metals onto ferric hydroxides minerals becomes significant. In this geologic setting, ferric hydroxides may adsorb heavy metals and help limit or diminish their mobility downstream. A geochemical model thus provides a powerful assessment of the effects of bacteria sulfate reduction on mineral precipitation and surface adsorption reaction.

MATERIALS AND METHODS

Injection Experiments

At the field site, we hypothesized that the SRB were dormant and lacked some metabolism-limiting nutrients in the

M.-K. Lee and J.A. Saunders, Department of Geology and Geography, 210 Petrie Hall, Auburn University, Auburn, AL 36849. Received 8 Aug. 2002. Special Submissions—Contaminant Characterization, Transport, and Remediation in Complex Multiphase Systems. *Corresponding author (leeming@auburn.edu).

Published in Vadose Zone Journal 2:177–185 (2003).

Abbreviations: DIRB, dissimilatory iron-reducing bacteria; EDAX, energy-dispersive x-ray analysis; Eh, redox potential; HFO, hydrous ferric oxide; ICP-MS, inductively coupled plasma mass spectrometry; SEM, scanning electron microscope; SRB, sulfate reducing bacteria.

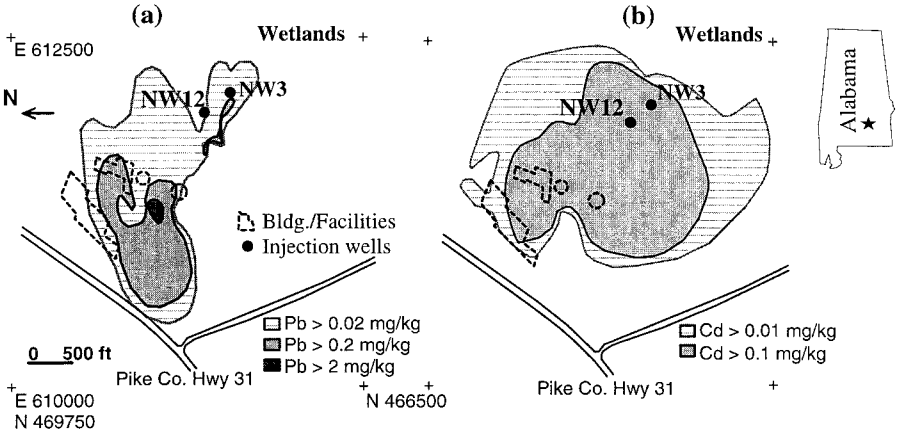

Fig. 1. Observed (a) Pb and (b) Cd plumes at Troy site in 1998. Also shown are locations of Injection Wells NW3 and NW12. Groundwater generally discharges in the southeast direction toward a wetland.

shallow aquifer. In the first test, performed 16 Dec. 1999, 45 kg (100 pounds) of sucrose (commercial grade), 2.25 kg (5 pounds) of diammonium phosphate [$(NH_4)_2HPO_4$], and 0.95 m^3 (250 gallons) of water (herein called the CNP solution for the elements added) were mixed in a plastic tank and added by gravity injection into an existing monitoring well, Well NW3 (Fig. 1), screened in a shallow sand aquifer. In the second test, performed 19 Sept. 2000, a mixture of 3.78 m^3 (1000 gallons) of water, 450 kg (1000 pounds) of sucrose, and 22.5 kg (50 pounds) of diammonium phosphate was injected into Well NW12 (Fig. 1). The first pilot experiment lasted only 2 mo, and the second test lasted for almost 1 yr to monitor the long-term changes of water chemistry during bioremediation. The injection water for both experiments was raw groundwater pumped from the Cretaceous Tuscaloosa aquifer from a Troy municipal well before chlorination. The injection water had low total dissolved solids (≈300 mg L^{-1}) and sulfate concentration (5–19 mg L^{-1}). The elevated alkalinity (135–166 mg L^{-1}) and "rotten egg" smell of H_2S of the injection water indicated the bacteria sulfate reduction in the deep Cretaceous aquifer (Penny, 2002).

Geochemical Analysis

Groundwater geochemical changes (major ions, trace elements, pH, Eh) were monitored in the injection wells during the experiments. Temperature, pH, oxidation–reduction potential, and electrical conductivity were measured in the field using hand-held water quality probes. Raw and acidified water samples and their replicates were sent to ACTLABS and University of Georgia for major ion and trace element analysis using inductively coupled plasma mass spectrometry (ICP-MS). Samples for trace element and cation analyses were passed through a 0.45-μm filter, acidified with concentrated HNO_3, and stored in polyethelene bottles. The $\delta^{34}S$ ratio of dissolved sulfate in groundwaters was measured before injection and carefully monitored after the injection when Eh drops below −100 mV. Sulfate reducing bacteria have a well-known kinetic isotope fractionation effect on dissolved sulfate and resulting biogenic hydrogen sulfide (Thode et al., 1951; Ehrlich, 1997). Because ^{32}S–O bonds are broken more easily than ^{34}S–O bonds during sulfate reduction, the H_2S generated is enriched in ^{32}S compared with the sulfate. Thus S isotopic signatures may be used to track the progress of bacteria sulfate reduction in groundwater.

Geochemical Modeling

In general, a geochemical model traces how a fluid's chemistry evolves and which minerals precipitate or dissolve over the course of a geochemical process. Construction of geochemical models for metal remediation requires the inclusion of surface complexation theory (i.e., Stumm and Morgan, 1981; Dzombak and Morel, 1990; Stumm, 1992) to account for the ion adsorption–desorption processes. General mathematical and numerical models for tracing water–rock interaction and sorption of dissolved metals onto mineral surface are well described by a number of investigators (e.g., Bethke, 1996; Lichtner, 1996; Van Cappellen and Wang, 1996). Here we briefly summarize how the surface complexation theory can be integrated into the equilibrium model of a multicomponent geochemical system.

The independent reactions between surface complex (A_q) and the basis species is

$$A_q = \nu_{wq}A_w + \sum_i \nu_{iq}A_i + \sum_k \nu_{kq}A_k + \sum_m \nu_{mq}A_m + \sum_p \nu_{pq}A_p \quad [1]$$

(Bethke, 1996), here ν_{wq} is the number of moles of water A_w in the reaction to form A_q, ν_{iq}, ν_{kq}, ν_{mq}, and ν_{pq} are the number of moles of the basis species A_i, minerals A_k, gases A_m, and uncomplexed surface sites A_p. The basis species A_i are a set of aqueous species required to identify each independent chemical reaction that can occur in a geochemical system. The molality of each surface complex (m_q) can be evaluated by the general mass action equation

$$m_q = \frac{1}{U_q e^{z_q F\Psi/RT_k}}\left(a_w^{\nu_{wq}} \prod^i (\gamma_i m_i)^{\nu_{iq}} \prod^k a_k^{\nu_{kq}} \prod^m f_m^{\nu_{mq}} \prod^p m_p^{\nu_{pq}}\right) \quad [2]$$

Here, a_w and a_k are the activity for water and minerals k, γ_i and m_i are the activity coefficient and molality for basis species i, f_m is fugacity for gases m, and m_p is molality for uncomplexed surface sites p. The equilibrium constant K for the surface complexation reaction includes both the chemical free energy (U_q) and electrostatic effects ($e^{z_0 F\Psi/RT_k}$, termed *Boltzman factor*). The mass balance equation for each surface site type is

$$M_p = n_w\left(m_p + \sum_q \nu_{pq}m_q\right) \quad [3]$$

This equation calculates the total number of sites M_p from the number of uncomplexed sites m_p and the surface complexes m_q in the mass n_w of solvent water. A mass balance equation can be derived for each chemical component, including the various surface sites, in the geochemical system. The system's equilibrium state and surface complexation reactions thus can be solved by substituting the mass action equations into the mass balance equations. Mass balance and mass action equa-

Table 1. Maximum contaminant levels (MCLs) for various elements present at the Sanders Lead site.

Contaminant	MCLs
	$\mu g\ kg^{-1}$
Pb	15
Cd	5
Fe	300
Al	50–200
SO_4	250 000
pH	6.5–8.5

tions for aqueous species, minerals, and gas are similar and are described in details by Bethke (1996). The Newton–Raphson method is used to solve iteratively a set of values for unknown variables from which secondary species can also be calculated.

Field Site

Groundwater at the site near Troy, AL (Fig. 1) was initially contaminated by Pb, Cd, Zn, and H_2SO_4 released in 1980s from a large car-battery recycling operation in southeastern Alabama, USA, which accounts for approximately 15% of the current U.S. lead production. Concentrations of several metals greatly exceed maximum contaminant levels suggested by USEPA (Table 1). Contaminated groundwater at the site occurs in a shallow, sandy water table aquifer containing abundant ferric oxyhydroxides (Saunders et al., 2001). Depth to the water table is typically about 5 m, and an underlying clay-rich confining layer occurs at a depth of about 12 m. Hydraulic conductivity of the aquifer ranges from 1.3×10^{-4} to 5.3×10^{-4} cm s^{-1}, and the average groundwater water is on the order of 3 cm d^{-1} (0.1 ft d^{-1}). Contaminated groundwater discharges southeastward toward a natural wetland and has caused extensive killing of natural vegetation at the site. A number of field treatment technologies for the removal of metals from groundwater have been used, including physical, chemical, and biological processes. A large-scale conventional pump-and-treat remediation operation has been ongoing for a decade with limited success in improving water quality. The pump-and-treat operations could have been severely hampered by geologic heterogeneity because low permeability zones can trap significant amounts of pollutants and later release them into the groundwater by desorption and diffusion (Lee et al., 2000). A natural groundwater discharge area near the site was turned into a constructed wetland designed to remove metals and neutralize acidity. This wetland approach improved water quality near the discharge zone but had little effect on attenuating major plumes near the source area. Our new bioremediation process involves the stimulation of naturally occurring SRB to remediate the metals-contaminated groundwater in situ. Although a full-scale in situ bioremediation may be also hampered by geologic complexity, it is very cost-effective and relatively simple to implement compared with pump-and-treat operations.

RESULTS

Groundwater Geochemistry Changes

For both injection experiments, groundwater acidity decreased with time from the initial addition of sucrose and diammonium phosphate to the wells. Groundwater in Wells NW3 and NW12 had an initial pH of 3.1 and 4.25 and had reached maximum pH values of 4.2 and 5.2, respectively, after the injection (Fig. 2a). Initial Eh values for groundwater in NW3 and NW12 wells were +400 and +125 mV, respectively. The Eh value for NW3 fell rapidly and dropped below −150 mV in the month after the nutrients injection. The Eh within Well NW12 fell slowly by comparison, but was also found to be dropping below −100 mV in just over 120 d.

A dramatic reduction in the concentrations of Pb and Cd were observed at both well sites (Fig. 2b and Fig. 3). Lead within Wells NW3 and NW12 fell from initial levels of 300 $\mu g\ kg^{-1}$ and 85 $\mu g\ kg^{-1}$, respectively, to less than 5 $\mu g\ kg^{-1}$, below the detection limit of ICP-MS. Cadmium concentrations fell from 450 and 240 $\mu g\ kg^{-1}$ for Wells NW 3 and NW 12, respectively, to $<5\ \mu g\ kg^{-1}$, below the detection limit. Similarly, other chalcophile ("sulfur-loving") elements (Cu, Zn) showed similar decreases (Fig. 2b and Fig. 3), consistent with all of these elements forming or coprecipitating in relatively insoluble sulfide phases. At both injection experiments the large reduction in Pb and Cd concentrations were accompanied by a lowering in sulfate concentration and the development of a new rotten egg smell characteristic of hydrogen sulfide produced by bacteria sulfate reduction. Early samples taken shortly after the injection had distinct alcohol odor characteristics of ethanol, and perhaps acetone and butanol, produced by fermentative microbes.

Concentration of Fe, however, increased significantly after injection of the CNP solution and did not drop to preinjection levels during the course of experiments (Fig. 2c). The Fe increase coupled with the moderately reducing conditions in the early stages of the experiment (Fig. 2a) indicate that the CNP solution might have initially stimulated indigenous dissimilatory iron-reducing bacteria (DIRB) to reductively dissolve solid Fe^{3+} phases in the aquifer and release Fe^{2+} to solution. The lack of a significant drop in Fe concentration after bacteria sulfate reduction began indicates that Fe was not precipitated as an abundant iron-sulfide phase in the early stage of the experiment. Similarly, siderophile ("iron-loving") elements Co and Ni showed no significant drop in concentration during the experiments (Fig. 2d). Concentrations of redox-sensitive elements U and Se decreased significantly as the Eh values dropped during the course of the experiments (Fig. 2e). Similarly, Al concentration also dropped during the course of the experiments (Fig. 2f), apparently due to pH increase, which probably caused precipitation of an aluminum hydroxide phase.

We observed a negative linear trend where dissolved sulfate became isotopically heavier as the sulfate content decreased (Fig. 4). Although observed fractionation was not great (maximum of approximately 0.5‰), the changing trend seems to be consistent with S isotope fractionation attending bacteria sulfate reduction. Bacteria reduction of sulfate leads to enrichment of ^{34}S in dissolved sulfate relative to H_2S because SRB preferentially use the lighter ^{32}S in generating H_2S gas. We compare the observed $\delta^{34}S$ change with theoretical fractionation using a mass balance calculation. In the calculation, the initial fluid is assumed to have a $\delta^{34}S = +6‰$ ($^{34}S/^{32}S$ ratio = 0.045 27) and the H_2S generated has a $\delta^{34}S =$

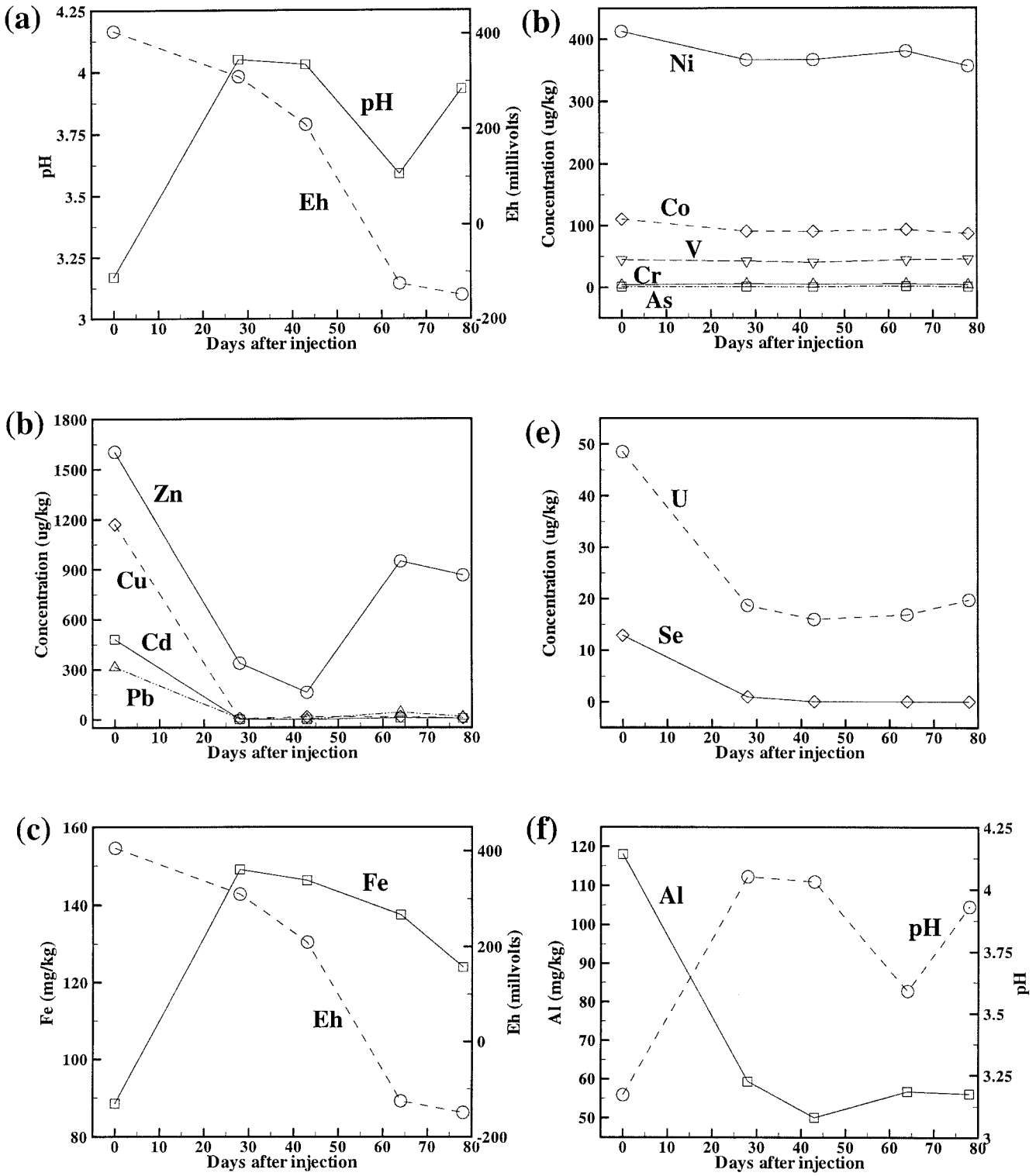

Fig. 2. Changes in geochemical parameters with time during the first injection experiment after the injection of sucrose and diammonium phosphate solution. (a) pH and Eh vs. time, (b) chalcophile elements (Zn, Cu, Cd, Pb) vs. time, (c) Fe and Eh vs. time, (d) siderophile elements (Ni, Co, V, Cr, As) vs. time, (e) redox-sensitive elements (U and Se) vs. time, and (f) Al and pH vs. time.

−20‰ ($^{34}S/^{32}S$ ratio = 0.044 10). Since approximately 25% of dissolved sulfate is reduced to H_2S during our experiment (Fig. 4), the final $\delta^{34}S$ value of fluid should approach +16‰ ($^{34}S/^{32}S$ ratio = 0.045 75), which is significantly higher than measured value (+6.6‰). This indicates that the fractionations imposed during the induced, high-rate sulfate reduction may be different from natural reduction systems with lower rates. Maximum fractionation has been observed in systems with low sulfate reduction rate, and vice versa (Rudnicki et al., 2001). Habicht and Canfield (1997) also indicated that the extent of isotopic fractionation depends on other

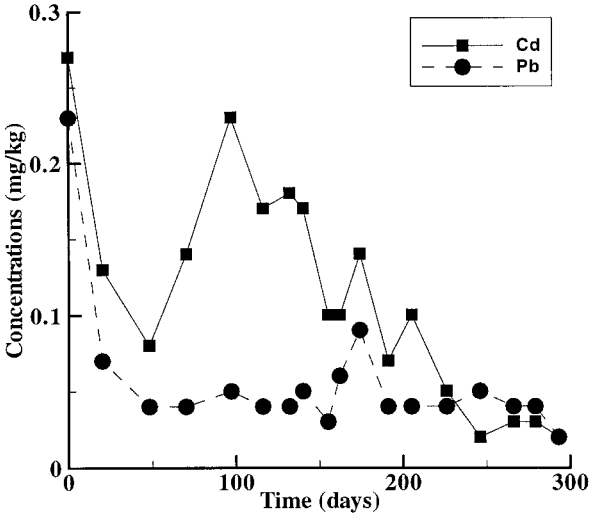

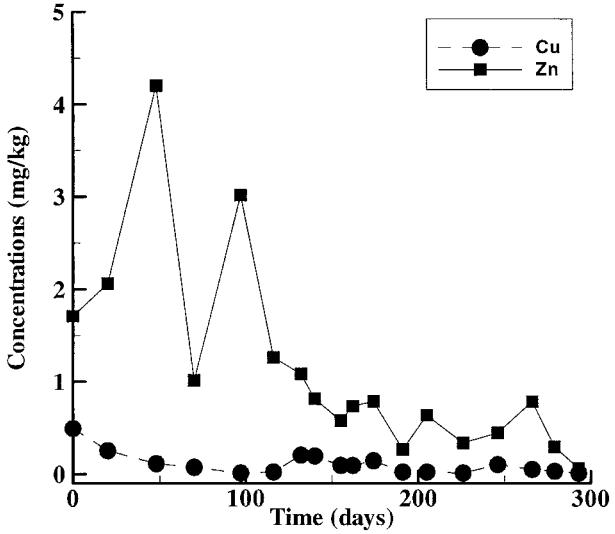

Fig. 3. Changes in chalcophile elements vs. time in the second injection experiment.

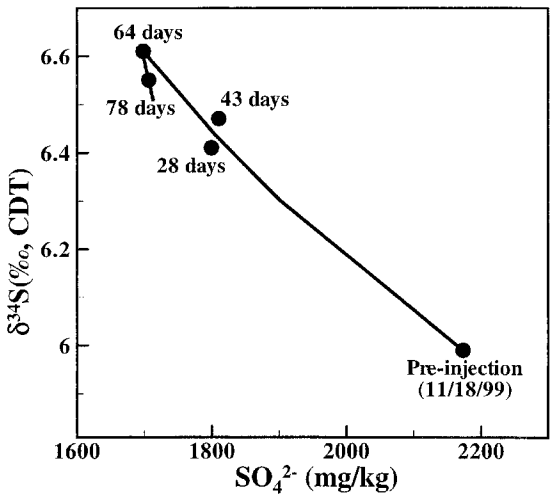

Fig. 4. Sulfur isotopic composition of dissolved sulfate concentration vs. sulfate concentration during bioremediation experiment.

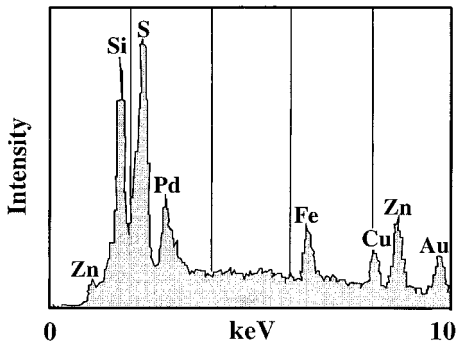

Fig. 5. Energy dispersive x-ray (EDAX) spectra of filtered materials from groundwater after bacteria sulfate reduction began.

factors such as sulfate concentration, pH, and bacteria population.

Solid Metal-Sulfide Precipitation

Water samples collected after injection no longer had their typical orange color from the suspended HFOs normal for an aerobic, Fe-rich water samples. Filters used on groundwater samples turned black, suggesting that metal-sulfide colloids were present in the water. Filters were first analyzed by x-ray diffraction, and they showed a diffuse and broad peak at Cu-Ka d-spacing of 3.12 Å, which is the principal ("100") peak for sphalerite (ZnS). Both extremely small grain size (nanocrystalline) and not completely biogenic crystalline phases can both cause the broad and diffuse x-ray diffraction peaks. Imaging of the filter surfaces with a scanning electron microscope (SEM) failed to reveal any obvious crystals, but energy-dispersive x-ray analysis (EDAX) of filtered material consistently resulted in peaks for Cu, Zn, Fe, and S, along with Al and Si (Fig. 5). Under the SEM, shrinkage cracks were obvious in the filtrate, suggesting that the Al and Si peaks represent amorphous "clay" precursors. Peaks for metals and S suggest that perhaps a single Fe-, Zn-, and Cu-S phase could be present, or more likely, mixed Cu-Fe-S and Zn-Fe-S phases given the results of x-ray diffraction data. Cadmium probably co-precipitates in much more abundant (from a mass balance standpoint), common sulfides such as Fe-S, Zn-S, Cu-S, and perhaps their mixed phases.

Geochemical Modeling Results

Geochemist's Workbench (Bethke, 1996; Lee and Bethke, 1996) was used to investigate how bacteria sulfate reduction induces the precipitation of metal sulfides from the contaminated groundwater. Calculations here are based on the thermodynamic database thermo.com. V8.R6.230 compiled at Lawrence Livermore National Laboratory and employ the extended Debye–Hückle method (Helgeson, 1969) for calculating activity coefficients. The calculations also predict the sorption of metals onto the surface the ferric oxide minerals present in the aquifer. The surface complexation reaction modeling was based on the double layer model presented by

Table 2. Chemical composition of contaminated groundwater used in geochemical modeling at 25°C. Sulfate concentration is adjusted to reflect charge balance.

Ion	Concentrations	Ion	Concentrations
	μg g^{-1}		μg kg^{-1}
Cl^-	590.0	Pb^{2+}	314.2
SO_4^{-2}	800.0	Cd^{2+}	480.4
Na^+	214.3	Zn^{2+}	1605.0
Ca^{2+}	163.6	Cu^+	1172.0
Mg^{2+}	13.4	Co^{2+}	110.5
K^+	3.2	Ni^{2+}	412.8
Al^{3+}	81.6	Cr^{3+}	3.8
Fe^{2+}	88.5	As^{3+}	2.0
Mn^{2+}	4.0	As^{5+}	2.0
Ba^{2+}	16.6	Se^{4+}	12.9
		Cs^+	3.2

Dzombak and Morel (1990). Table 2 shows the initial chemical compositions of metal-contaminated groundwater used in the simulation.

To calculate the effect of SRB metabolism processes, the fluid redox potential Eh decreases linearly from its initial values of +400 to −150 mV at the end of the reaction path, as observed in the field during bioremediation. To calculate how pH affects sorption of various metals onto ferric hydroxide [$Fe(OH)_3$], pH varies from 3.2 to 6 in a sliding activity path. The initial system contains 1 kg of fluid (Table 1, pH = 3.17) and a small amount (1 cm^3) of ferric hydroxide. More stable ferrite minerals hematite, goethite, and jarosite are suppressed and not considered in the simulation. Ferric hydroxides used in the simulation have high specific surface areas (600 $m^2\ g^{-1}$) and thus provides a large number of sites for sorption reactions. The surface of HFOs is composed of weakly sorbing site (density = 0.4 mol mol^{-1} mineral) and a lesser number of strongly sorbing sites (density = 0.01).

The modeling results show how the mobility of metals is affected by the geochemical changes (a drop in Eh and an increase in pH) induced by bacteria sulfate reduction. Sulfide produced by sulfate reduction react with metals to form minerals including pyrite (FeS_2), galena (PbS), sphalerite (ZnS), covellite (CuS), orpiment (As_2S_3), and others precipitate at Eh below −50 mV (Fig. 6). The precipitation of solid minerals significantly lowers the concentrations of corresponding metals in solution. Although precipitation of metal sulfide minerals in the natural system is not expected in a short time period, as

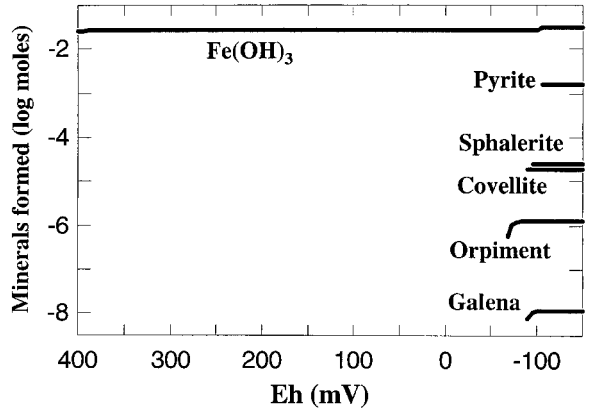

Fig. 6. Predictive cumulative mineral assemblage precipitated as Eh decreases as a result of bacteria sulfate reduction.

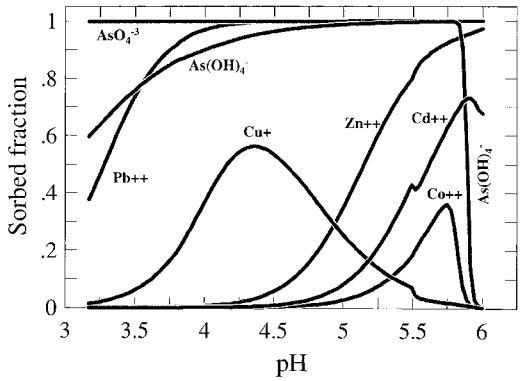

Fig. 7. Predictions of the amounts of metals present initially in contaminated water that sorb onto hydrous ferric hydroxides as a function of pH, calculated according to the Dzombak and Morel (1990) surface complexation model.

discussed above, the formation of metal-sulfide colloids observed (Fig. 5) agrees with the geochemical evolution predicted by the modeling.

Given the Fe-rich nature of the aquifer and groundwaters in this study, the site behaves from the biogeochemical standpoint like the "Fe-dominated" system as defined by Cooper and Morse (1998) for one type of anoxic marine environments. Under Fe-dominated conditions, the solid HFO phases behave as a sink for sulfide, by a reaction like this:

$$FeO(OH) + H_2S + 1/2H_2 \rightarrow FeS(am) + 2H_2O \quad [4]$$

Here FeS(am) is the kinetically favored precursor to the very common mineral pyrite (Schoonen and Barnes, 1991). At our site, reactive Fe phases in the aquifer have the effect of lowering the dissolved sulfide concentration below that necessary for precipitating FeS(am), but keeps it great enough to precipitate sulfides of the chalcophile elements. So pyrite would not form as predicted until SRB are stimulated to produce enough H_2S to first consume reactive solid Fe phases before precipitation of FeS(am).

The calculation also shows that various metals are sorbed over a wide range of pH during sulfate reduction (Fig. 7). Metal ions remain in solution as long as the pH is below 3.5. As the pH value increases over the reaction, sorption of metals on HFOs becomes significant in the reacting geochemical system. Dissolved Pb is strongly sorbed at relatively low pH (<4), which is consistent with its removal observed during the field remediation (Fig. 2 and 3). For As, arsenate sorbs strongly onto the protonated weak sites of ferric hydroxide for the entire range of calculation (Fig. 7):

$$(w)FeOH_2^+ + H_2AsO_4 \rightarrow (w)FeH_2AsO_4 + H_2O \quad [5]$$

Arsenite dominates at lower oxidation and low pH conditions, and its sorption is also favored by increasing pH according to

$$(w)FeOH_2^+ + As(OH)_3 \rightarrow (w)FeH_2AsO_3 + H_2O + H^+ \quad [6]$$

The modeling result indicates that As is increasingly sorbed onto the ferric hydroxide surface as pH increases under acidic condition. However, at very low oxidation

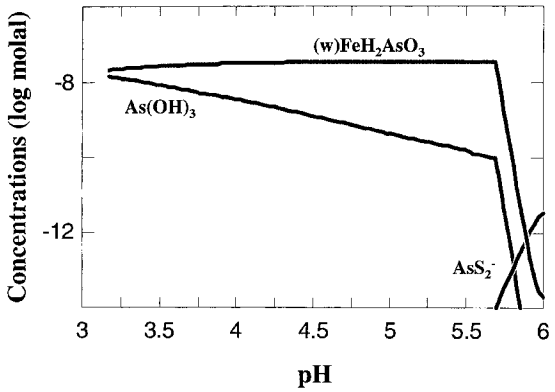

Fig. 8. Calculated mass of predominant As species of a reaction path in which arsenite sorbs onto ferric hydroxide to form FeH_2AsO_3 complexes as pH increases. The value of pH increases as a result of bacteria sulfate reduction. Arsenite later desorbs to form AsS complexes under reducing, neutral pH conditions.

state as pH increases to about 5.8, As desorbs (Fig. 7 and 8) and becomes mobilized as it reacts with dissolved sulfide to form AsS complexes.

Up to 20% of aqueous Cu can also be sorbed on HFOs in the early stages of low-pH condition, but it desorbs as pH continues to rise (Fig. 7). Copper desorbs as it loses competition with Co, Ni, and Zn for the strongly sorbing sites. Hydrous ferric oxides can preferentially scavenge Pb, As, and Cu from the solution because they have a high affinity for these metal ions (Table 3). The modeling result explains why the Pb plume is retarded in migration with respect to the Cd plume (Fig. 1) under the low-pH conditions. The sorption of Zn, Cd, Co, and Ni takes place only at relatively neutral or high pH conditions (Fig. 7) and thus has little effect in metal attenuation in our acidic setting.

The sorption of cations is promoted as pH increases for two reasons. First, in low pH environments, ferric hydroxide hold mainly protonated sites [e.g., $(w)FeOH_2^+$]. As a result, the surface maintains a net positive charge. The positive charge on mineral surface, however, gradually decreases as pH increases, thus reducing the electrical repulsion between sorbing surface and cations. Moreover, lower H^+ concentration also favors cation sorption by mass action. For example, the sorption of bivalent cations such as Cd^{2+} on HFOs can be written as

$$(s)FeOH_2^+ + Cd^{2+} \rightarrow (s)FeOCd^+ + 2H^+ \qquad [7]$$

Lowering H^+ concentration will drive this reaction toward the right-hand side and favor the sorption of Cd^{2+}

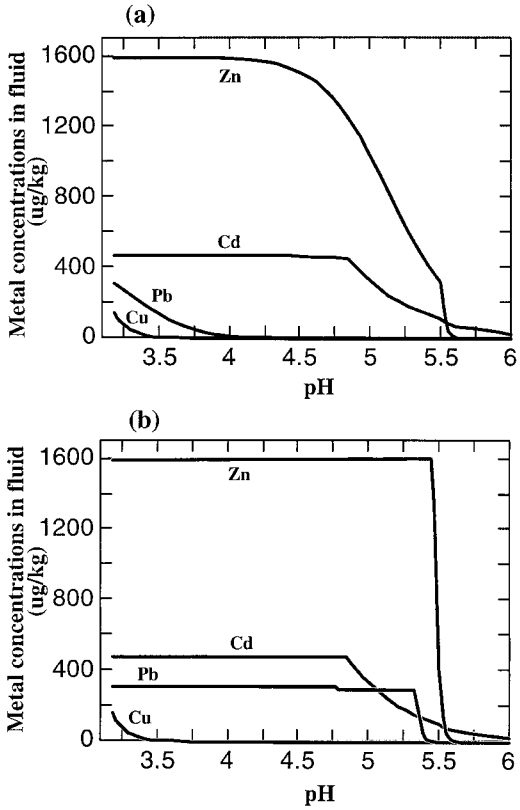

Fig. 9. The effect of sorption on metal attenuation. Diagrams compare (a) the concentration attenuation of metals which are sorbed with (b) the curves of the same metals without sorption effects.

by increasing pH. There is a similar pH effect for other bivalent cations.

The effects of sorption on chemical evolution of metals can be seen by comparing the results of a model that combines precipitation and sorption (Fig. 9a) and a model that considers only precipitation (Fig. 9b). Sorption effectively removes Pb in low pH conditions, as discussed above. Concentration curves of most metals in both models do not depart largely from each other. It is apparent that Zn and Cd are removed mainly by direct precipitation of sulfide solids via bacteria sulfate reduction processes.

DISCUSSION

This study shows that primary geochemical controls governing the bioremediation of metals-contaminated groundwater at the site include mineral precipitation or

Table 3. Selected surface complexation reactions and equilibrium constants considered in geochemical modeling.

Chemical reactions	Equilibrium constants (log K)
$(w)FeOH$† $+ AsO_4^{3-} + 3H^+ \rightarrow (w)FeH_2AsO_4 + H_2O$	29.31
$(s)FeOH + Cu^+ + 0.25O_2(aq) \rightarrow (s)FeOCu^+ + 0.5\,H_2O$	21.67
$(w)FeOH + As(OH)_3 \rightarrow (w)FeH_2AsO_3 + H_2O$	5.41
$(s)FeOH + Pb^{2+} \rightarrow (s)FeOPb^+ + H^+$	4.65
$(s)FeOH + Zn^{2+} \rightarrow (s)FeOZn^+ + H^+$	0.99
$(s)FeOH + Cd^{2+} \rightarrow (s)FeOCd^+ + H^+$	0.47
$(s)FeOH + Ni^{2+} \rightarrow (s)FeONi^+ + H^+$	0.37
$(s)FeOH + Co^{2+} \rightarrow (s)FeOCo^+ + H^+$	−0.46

† The strong and weak sorbing sites are labeled as (s)FeOH and (w)FeOH, respectively.

adsorption of metals on the surface of HFOs. Redox potential and pH are the most important factors controlling metal speciation, precipitation, and sorption. Toxic metals are soluble and mobile in aerobic, acidic groundwater, as those present at our study site or similar acid mine drainage sites. Field data demonstrated that the indigenous SRB in a metal-contaminated aquifer were capable of anaerobically catalyzing sulfate reduction to form insoluble metal sulfide solids. This bioremediation process diminishes and limits the spreading of metals to nearby water resources. Geochemical evolution of groundwater during bioremediation is consistent with removal of two principal metals (Pb and Cd) and other chalcophile elements as solid Zn, Pb, and Cu sulfide phases. Given the similar geochemical behavior of Zn and Cd, it is likely that Cd would not have formed a separate sulfide phase, but would have coprecipitated in sphalerite. In both experiments, our anaerobic processes were effective at removing chalcophile and pH-sensitive elements, but failed at siderophile elements (e.g., Fe, Co, Ni). It is unclear whether the disparity in effectiveness reflects the fundamental geochemical differences between chalcophile and siderophile elements or is the result of our water filtering procedures (i.e., FeS colloids may or may not pass through filter pores depending on their size).

The broad and diffuse x-ray diffraction peaks for sphalerite indicate that these biogenic sulfides exist as extremely small grains or nanocrystallines. Transmission electron microscopy analysis of the biogenic sphalerite grains in similar studies (e.g., Labrenz et al., 2000; Banfield et al., 2000) also show them to be aggregates of nanoscale microspherulites. High surface area of nanocrystallines and their aggregate texture could greatly enhance the chemical reaction rates and facilitates metal precipitation and sorption. These solid phases are probably colloidal on precipitation during bioremediation. Wetland vegetation down gradient from the heavily contaminated sites could help trap such small particles.

Our study implies that the injected solution could induce indigenous bacteria to precipitate "bio-minerals" phases (crystalline and amorphous) as in situ filters for long-term remediation in the aquifer volume surrounding the well. Even when the C source is exhausted or when the aquifer redox conditions fluctuate, these reduced (sulfides) and oxidized (such as iron and manganese oxides or oxyhydroxides) mineral phases have the capacity to remove toxic heavy metals and metalloids by sorption on mineral surfaces and also by coprecipitation (i.e., contaminants incorporated into the solid mineral phases during continued growth).

Geochemical modeling is used to demonstrate the relative importance of mineral precipitation and sorption on the attenuation of metal contaminants. Modeling results show that solid sulfide phase precipitation apparently removes most aqueous Zn, Pb, and Cu, whereas both sorption (due to pH increase) and sulfide formation were important for removing Pb. Ferric hydroxides in the aquifer have a high affinity for aqueous metal species. Sorption acts as an important metal scavenger for Pb; however, it does not play a significant role for removing Co, Ni, and Cd in acidic environments such as our site. The plumes of Pb and Cd observed in 1998 clearly show this "chromatographic" (i.e., separation of the components of plume) effect of retardation (Fig. 1). The Cd, which is not sorbed at low pH environments, can be seen to have moved significantly down gradient beyond the strongly sorbed Pb. Modeling results also show that competition for the strongly sorbing sites may lead to the desorption of certain ions (such as Cu) at neutral pH conditions. Our field data indicate that percolating of rainfall through the aquifer could cause short-term Eh increases, potentially leading to oxidation of sulfide solids and subsequent pH decrease, and the remobilization of metals. Thus it is important to consider Eh and pH changes and related factors when evaluating the fate, transport, and long-term stability of metals at shallow contaminated sites.

Modeling results have implications for remediating other sites where natural geochemical processes release heavy metals and contaminate water supplies. For example, the scope of the natural As contamination had been recognized in alluvial aquifers worldwide (e.g., Bangladesh, West India) since early 1990s (Bagla and Kaiser, 1996; Nickson et al., 1998). Our modeling result is consistent with the hypothesis (e.g., Nickson et al., 2000; McArthur et al., 2001) that As is strongly sorbed by HFO under oxidized conditions, and the subsequent HFO (bacteria) reductive dissolution mechanism might be an important process contributing to the problem. We hypothesize that deposition of stream sediments containing HFOs and organic matter in alluvial deposits ultimately triggers the activity of dissimilatory Fe^{3+}-reducing bacteria, resulting in the release of sorbed As to groundwater. Our modeling result shows that As is distinctive in being relatively mobile by desorption processes under reduced, neutral pH conditions. However, high As concentrations are not expected in S-rich, acidic, reducing system since such geochemical environments favor the precipitation of sulfide minerals (i.e., orpiment, realgar, Fig. 6) that contain As.

This study demonstrates that careful geochemical modeling can provide a better understanding of the biogeochemical cycle and mobility of metals in alluvial aquifers. Development of a successful full-scale bioremediation operation requires (i) a well-prepared, detailed site characterization to allow the reliable prediction of the field remediation effectiveness and (ii) an integrated geochemical and microbiological analyses, combined with theoretical modeling for the assessment of the progress of subsurface bioremediation.

ACKNOWLEDGMENTS

This research was supported by grants from USGS-WRRI, Alabama-ADECA, and by the Petroleum Research Fund, administered by the American Chemical Society under ASC-PRF 37071-AC2 (to Ming-Kuo Lee). We thank Chris Rutherford (Sanders Lead) for field assistance and helpful discussions.

REFERENCES

Bagla, P., and J. Kaiser. 1996. India's spreading health crisis draws global arsenic experts. Science 274:174–175.

Banfield, J.F., S.A. Welch, H. Zhang, T.T. Ebert, and R.L. Penn. 2000. The role of aggregation in crystal growth and transformations in nanophase FeOOH biomineralization products. Science 289: 751–754.

Berner, R.A. 1970. Sedimentary pyrite formation. Am. J. Sci. 268:1–23.

Bethke, C.M. 1996. Geochemical reaction modeling. Oxford University Press, New York.

Bottrell, S.H., P.J. Hayes, M. Nannon, and G.M. Williams. 1995. Bacteria sulfate reduction and pyrite formation in a polluted sand aquifer. Geomicrobiol. J. 13:75–90.

Chapelle, F.H. 1993. Groundwater microbiology and geochemistry. John Wiley & Sons, New York.

Cooper, D.C., and J.W. Morse. 1998. Biogeochemical controls on trace metal cycling in anoxic marine sediments. Environ. Sci. Technol. 32:327–330.

Dzombak, D.A., and F.M.M. Morel. 1990. Surface complexation modeling: Hydrous ferric oxide. John Wiley & Son, New York.

Edwards, K.J., P.L. Bond, T.M. Gihring, and J.F. Banfield. 2000. An archaeal iron-oxidizing acidophile important in acid mine drainage. Science 287:1796–1798.

Ehrlich, H.L. 1997. Geomicrobiology. Marcel Dekker, New York.

Elliott, P., S. Ragusa, and D. Catcheside. 1998. Growth of sulfate-reducing bacteria under acidic conditions in an upflow anaerobic bioreactor as a treatment system for acid mine drainage. Water Res. 32:3724–3730.

Habicht, K.S., and D.E. Canfield. 1997. Sulfur isotope fractionation during bacteria sulfate reduction in organic rich sediments. Geochim. Cosmochim. Acta 61:5351–5361.

Helgeson, H.C. 1969. Thermodynamics of hydrothermal systems at elevated temperatures and pressures. Am. J. Sci. 267:729–804.

Helgeson, H.C., T.H. Brown, A. Nigrini, and T.A. Jones. 1970. Calculation of mass transfer in geochemical processes involving aqueous solution. Geochim. Cosmochim. Acta 34:569–592.

Labrenz, M., G.K. Druschel, T. Thomsen-Ebert, B. Gilbert, S.K. Welch, K. Kemner, G.A. Logan, R. Summons, G. De Stasio, P.L. Bond, B. Lai, S.D. Kelley, and J.F. Banfield. 2000. Natural formation of sphalerite (ZnS) by sulfate-reducing bacteria. Science 290:1744–1747.

Lee, M.-K., and C.M. Bethke. 1996. A model of isotopic fractionation in reacting geochemical systems. Am. J. Sci. 296:965–988.

Lee, M.-K., J.A. Saunders, and L.W. Wolf. 2000. Effects of geologic heterogeneities on pump-and-treat and in situ bioremediation: A stochastic analysis. Environ. Eng. Sci. 17:183–189.

Lichtner, P.C. 1996. Continuum formulation of multicomponent-multiphase reactive transport. p. 1–79. *In* P.C. Lichtner et al. (ed.) Reactive transport in porous media. Reviews in Mineralogy 34. Mineralogical Soc. Amer., Washington, DC.

McArthur, J.M., P. Ravenscroft, S. Safiulla, and M.F. Thirlwall. 2001. Arsenic in groundwater: Testing pollution mechanisms for sedimentary aquifers in Bangladesh. Water Resour. Res. 37:109–117.

Nickson, R.T., J.M. McArthur, W.G. Burgess, K.M. Ahmed, P. Ravenscroft, and M. Rahman. 1998. Arsenic poisoning of Bangladesh groundwater. Nature 395:338.

Nickson, R.T., J.M. McArthur, P. Ravenscroft, W.G. Burgess, and K.M. Ahmed. 2000. Mechanism of arsenic release to groundwater, Bangladesh and West Bengal. Appl. Geochem. 15:403–414.

Parkhurst, D.L., D.C. Thorstenson, and L.N. Plummer. 1990. PHREQE-A computer program for geochemical calculations. U.S. Geol. Surv. Water Res. Invest. 80-96. U.S. Geol. Surv., Reston, VA.

Penny, E.A. 2002. Groundwater geochemistry, isotope hydrology, and microbiology of Alabama coastal plain aquifers. M.S. thesis, Auburn University, Auburn, AL.

Postgate, J.R. 1979. The Sulphate-reducing bacteria. Cambridge University Press, Cambridge, UK.

Reed, M.H. 1982. Calculation of multicomponent chemical equilibria and reaction processes in systems involving minerals, gases, and an aqueous phase. Geochim. Cosmochim. Acta 46:513–528.

Rudnicki, M.D., H. Elderfield, and B. Spiro. 2001. Fractionation of sulfur isotopes during bacteria sulfate reduction in deep ocean sediments at elevated temperatures. Geochim. Cosmochim. Acta 65:777–789.

Saunders, J.A., M.-K. Lee, J.M. Whitmer, and R.C. Thomas. 2001. In situ bioremediation of metals-contaminated groundwater using sulfate-reducing bacteria: A case study. p. 105–112. *In* A. Leeson et al. (ed.) Proc. Int. Symposium on In-Situ and On-Site Bioremediation, 6th. Vol. 6(9). Battelle Press, San Diego, CA.

Schoonen, M.A.A., and H.L. Barnes. 1991. Reactions forming pyrite and marcasite from solution: I. Nucleation of FeS_2 below 100°C. Geochim. Cosmochim. Acta 55:1496–1504.

Stumm, W. 1992. Chemistry of the Solid-Water Interface. Wiley, New York.

Stumm, W., and J.J. Morgan. 1981. Aquatic chemistry, An introduction emphasizing chemical equilibria in natural waters. 2nd ed. Wiley, New York.

Thode, H.G., H. Kleerekoper, and D. McElcheran. 1951. Isotope fractionation in the bacteria reduction of sulfate. Research (London) 4:581–582.

Wolery, T.J. 1979. Calculation of chemical equilibrium between aqueous solution and minerals: The EQ3/6 software package. Report UCRL-52658. Lawrence Livermore National Laboratory, Livermore, CA.

Van Cappellen, P., and Y. Wang. 1996. Cycling of iron and manganese in surface sediments: A general theory for the coupled transport and reaction of carbon, oxygen, nitrogen, sulfur, iron, and manganese. Am. J. Sci. 296:197–243.